Cross-Coupled Microstrip Filter Using Grounded Patch Resonators

Vasa Radonic and Vesna Crnojevic-Bengin
University of Novi Sad, Faculty of Technical Sciences
Novi Sad, Serbia
vasarad@uns.as.rs, bengin@uns.ac.rs

Abstract—**In this paper, a new cross-coupled microstrip filter based on the grounded patch resonators is designed, fabricated and measured. Coupling characteristics of three basic coupling structures encountered in this class of filters are investigated using full-wave electromagnetic simulations, and the design curves for coupling coefficients and the external quality factor are presented. As the demonstration, a fourth order cross-coupled filter of this type is designed, fabricated and measured.**

Keywords- cross-coupled filter; patch resonator, microstrip.

I. INTRODUCTION

Compact microwave bandpass filters are greatly needed for modern communication systems which demand small size and light weight. High performance narrow-band microstrip filters with low insertion losses, high selectivity and linear phase or flat group delay in the pass band are essential, especially in satellite and mobile communication systems.

The filters based on modified Chebyshev-type characteristic with additional transmission zeros at finite frequencies have been developed by various authors in order to meet these specifications, [1-6]. Typically, such quasi-elliptic response filters are realized by exploiting coupling between non-adjacent resonators. Several new cross-coupled planar filters have been proposed based on different resonator geometries, such as square open-loop resonators, [3], the hairpin resonator, [4], triangular open loop resonators, [5], or fractal resonators, [6].

In this paper, we propose cross-coupled filter based on square grounded patch resonators. The fabrication of the grounded patch is less sensitive to dimension tolerances in contrast to resonators previously reported in the literature, since it does not require narrow conductive lines. In the same time, they are very compact in size and exhibit low insertion loss. The grounded patch resonator was initially proposed in the design of two-dimensional high-impedance surfaces, [7], but was seldom used in microstrip filter design. Recently, we have used the grounded patch specifically coupled to the microstrip line to design extremely compact stopband filters, [8], and multi-band resonators [9]. In this paper, we use modified square grounded patch to design highly-selective compact cross-coupled filters following the coupling coefficient design approach, [3]. After detailed description of the resonator, the design curves for coupling coefficients and the external quality factor are presented. To demonstrate the validity of the approach, a prototype filter of fourth order is fabricated and measured.

II. GROUNDED PATCH RESONATOR

The grounded patch comprises of a metal square etched on the top side of the substrate, connected by a central via to the ground plane on the lower side of the substrate. In the modified version which we propose in this paper, the via is shifted to the side of the metal patch. In this way, electric, magnetic and mixed coupling can be achieved between adjacent resonators, as will be shown later.

The proposed resonator capacitively coupled to the feed lines is shown in Fig. 1, where a is side of the square patch, d is dimension of the square via, and g is a gap between the feeds and the resonators. The size of the patch was chosen to be a=6 mm, while d=0.4 mm and g=0.1 mm. The circuit is realized on a 1.27 mm thick Taconic CεR-10 substrate, with ε_r=9.8 and dielectric loss tangent equal to 0.0035. Conductor losses are modeled using bulk conductivity for copper. All simulations were performed using EMSight, full-wave simulator from Microwave Office. Response of the proposed resonator is shown in full lines in Fig. 2.

The resonator exhibits first resonance at f_r=2.85 GHz, while the second one occurs at 2.6 f_r. To understand its behavior, the resonator has been modeled with an equivalent circuit shown in Fig. 3 where L_v represents the via inductance, C_p is patch capacitance towards the ground, L_p is the series inductance of the patch and C_g models the capacitance between the feeds and the resonator. The extracted element values are: C_g=0.121 pF, L_p=0.74 nH, L_v=0.683 nH, C_p=2.311 pF. The response of the model, shown in dashed line in Fig. 2, exhibits good agreement with the EM one. It can be concluded that the first resonant frequency is determined by the shunt inductance L_v and the shunt capacitance C_p, while the second one depends on the serial inductance L_p and shunt capacitance C_p. The second resonant frequency is the same as that of the conventional half-wavelength resonator realized using the same patch but without the via, and can be easily shifted towards higher frequencies by changing the length of the patch or the substrate thickness. Accordingly, it is clear that the grounded patch is suitable for the design of bandpass filters with extended stopband region.

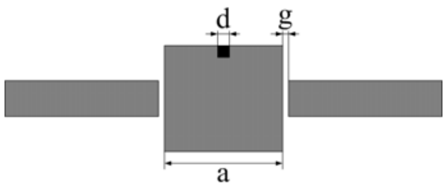

Figure 1. Proposed grounded patch resonator.

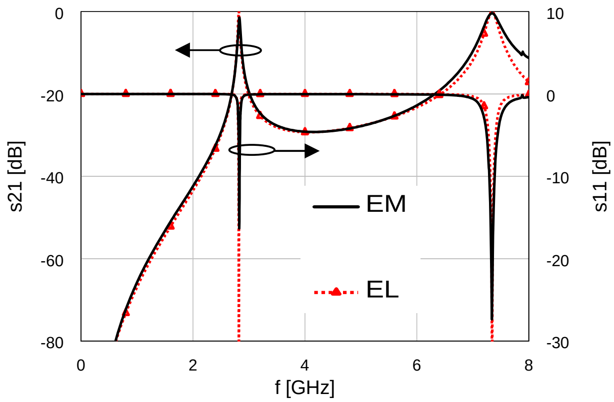

Figure 2. Full-wave simulated response of the grounded patch resonator and the response of the circuit model.

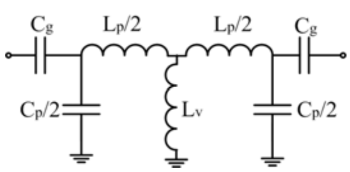

Figure 3. Equivalent circuit of the proposed resonator.

III. Coupling Structures

Due to the specific resonator design, where the via is shifted to one side of the metal patch, three basic coupling structures can be realized, Fig. 4. They result from different orientations of identical grounded patch resonators, which are separated by spacing s and may be shifted for an offset d. The nature and the intensity of the fringing fields in those three geometrical arrangements determine the nature and the strength of the coupling: the maximum magnetic coupling is obtained when the vias are placed close to each other, Fig. 4a, while the electric coupling exists when ''free'' sides of the patches are in proximity, i.e. when the vias are placed on the opposite sides of the patches, Fig. 4b. Mixed coupling refers to the structure proposed in Fig. 4c, since both electric and magnetic coupling occur in that case.

Fig. 5 shows transmission characteristics for structures with electric and magnetic coupling, together with corresponding phase responses. In both cases the distances s is equal to 1.2 mm. It can be seen that the magnetic coupling is stronger than the electric one, for the same distance s. In addition, it can be seen that the phase characteristics are out of phase, an evidence that two coupling coefficients will have opposite signs.

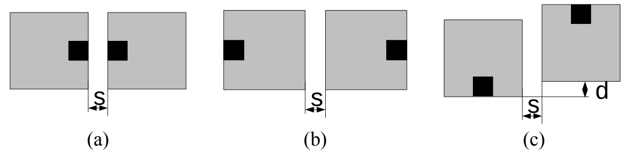

Figure 4. Basic coupling structures of coupled grounded patch resonators: (a) magnetic coupling, (b) electric coupling, (c) mixed coupling.

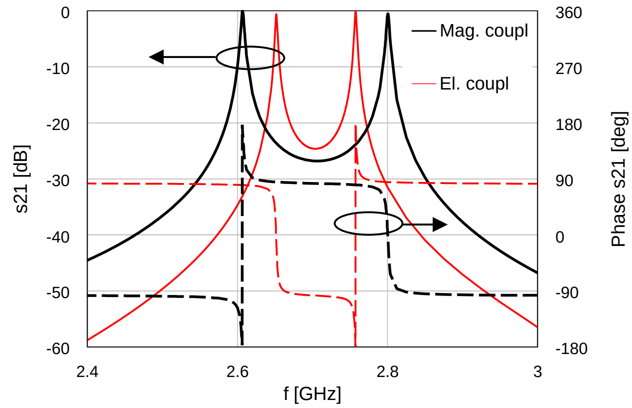

Figure 5. Comparison of electric and magnetic coupling responses.

To design cross-coupled filters based on the proposed resonator, values of coupling coefficients are needed for various resonator-to-resonator distances, s. The coupling coefficient k can be calculated from two split resonant frequencies f_1 and f_2, obtained from full-wave EM simulations of two over-coupled resonators, [3], using:

$$k = \frac{f_2^2 - f_1^2}{f_2^2 + f_1^2}. \tag{1}$$

The obtained coupling coefficients as a function of resonator-to-resonator distance s and offset d are shown in Fig. 6. As expected, the mixed coupling results in the smallest values of coupling coefficient. Also, it can be noted that in the case of mixed coupling variation of offset d has very small influence to the coupling coefficient k_{MIX}.

Similarly, the external quality factor was determined as a function of the coupling line length l, Fig. 7. For $l<a$, the coupling line lies only above the resonator, while for $a<l<2a$, it extends to the resonator's side as well, as shown in an inset of Fig. 7. Fine tuning of the external quality factor can be obtained by changing the feed line position t, Fig. 8.

IV. Filter Design

To demonstrate the validity of the approach, bandpass filter of the fourth order with the coupling structure shown in Fig. 9 has been designed, fabricated and measured. The filter has been designed to the following specifications: central frequency f_c=2.85 GHz, fractional bandwidth FBW=5 %, and two transmission zeros positioned at 2.85±0.15 GHz. The generalized equivalent network of the prototype is shown in Fig. 10 where J and g denote admittance inverters and capacitances, respectively. The values of g_i and J_i have been calculated using synthesis equation in [3]. For the fourth order filter with return loss L_R=-20 dB and frequency allocation of the transmission zeros Ω=1.82, the calculated values are: g_1=0.95914, g_2=1.4169, J_1=-0.20509, and J_2=1.1105.

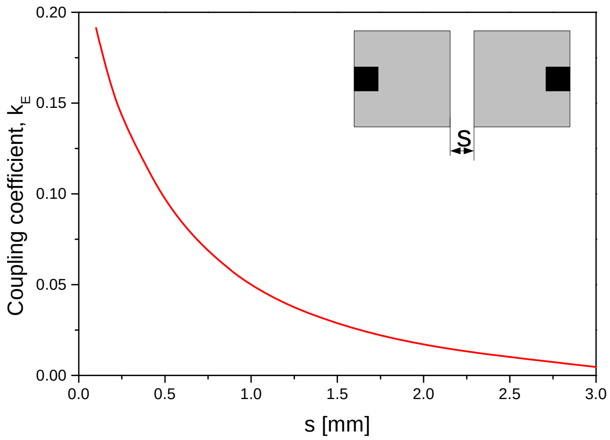

(a)

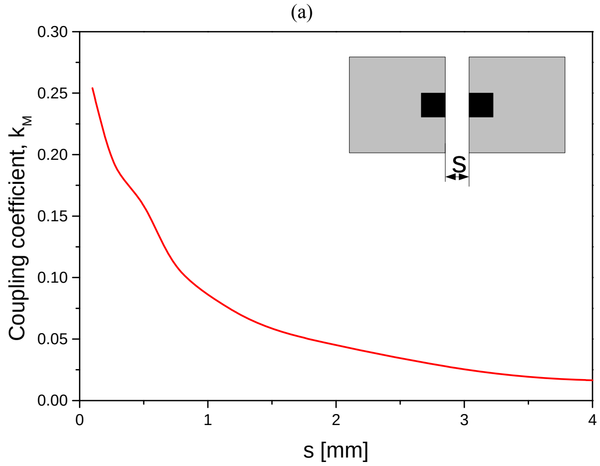

(b)

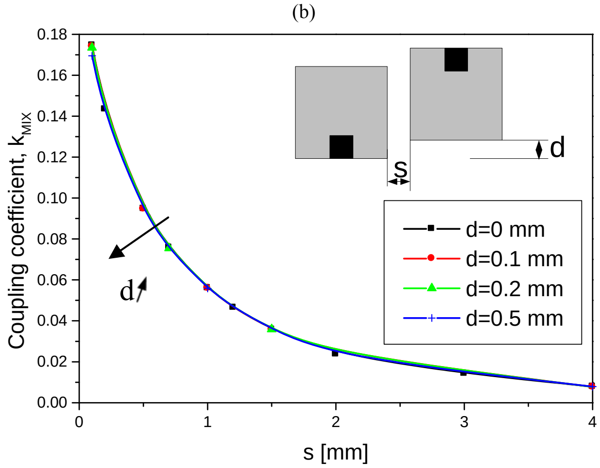

(c)

Figure 6. Coupling coefficients versus resonator-to-resonator distance *s* for: (a) electric coupling, (b) magnetic coupling, (c) mixed coupling (dependence from an offset *d* is also shown, as *d* is increased).

Those values can be used to calculate external quality factor and coupling coefficients using the following:

$$Qei = Qeo = \frac{g_1}{FBW}, \tag{2}$$

$$M_{1,2} = M_{3,4} = \frac{FBW}{\sqrt{g_1 g_2}}, \tag{3}$$

$$M_{2,3} = \frac{FBW \cdot J_2}{g_2}, \tag{4}$$

$$M_{1,4} = \frac{FBW \cdot J_1}{g_1}. \tag{5}$$

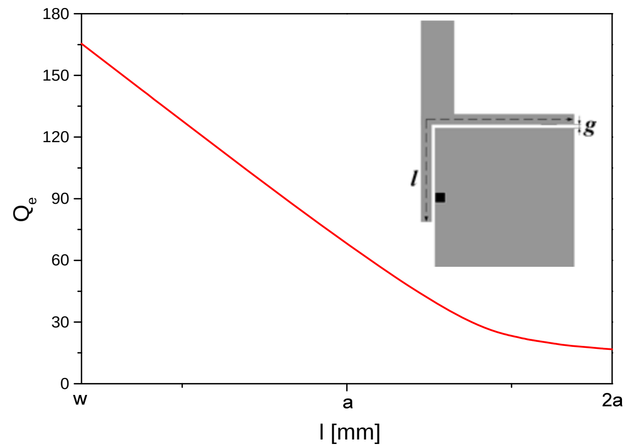

Figure 7. External quality factor as a function of the coupling line length *l*.

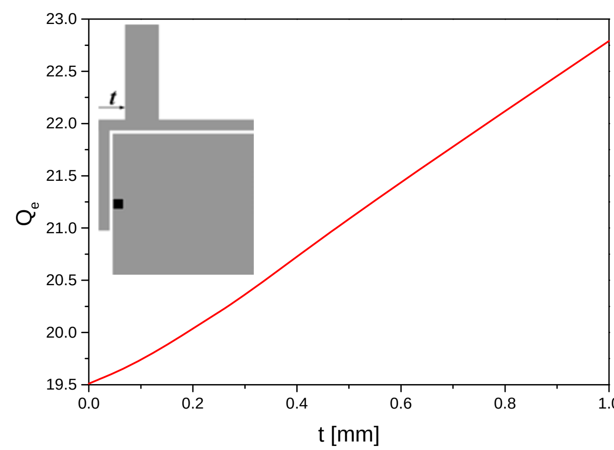

Figure 8. Fine tuning of the external quality factor by changing the position of the feed line, *t*, for fixed length of the coupling line *l*=11.2 mm.

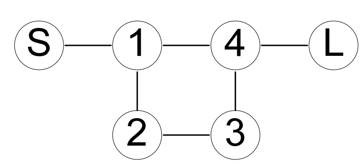

Figure 9. Coupling structure of the proposed filter.

To achieve desired values of M_{14}, M_{23} and M_{12}, three coupled pairs with electric, magnetic and mixed coupling are empolyed, respectively. Positive coupling coefficients M_{12}=M_{34} and M_{23} are realized by the mixed and magnetic coupling, respectively, while the negative coupling coefficient M_{14} is realized using the electric coupling. The coupling matrix is:

$$[M]=\begin{bmatrix} 0 & 0.0428903 & 0 & -0.0106913 \\ 0.0428903 & 0 & 0.0391877 & 0 \\ 0 & 0.0391877 & 0 & 0.0428903 \\ -0.0106913 & 0 & 0.0428903 & 0 \end{bmatrix} \quad (6)$$

Using the design curves given in Section III, all dimensions of the filter, such as spacings and the feed location were determined. The spacings between the resonators are s_{14}=2.51 mm, s_{23}=2.27 mm and s_{12}=1.305 mm for offset d=0.1 mm. Since the actual line widths and spacing are determined by the resolution of the PCB technology, we set them to s_{14}=2.5 mm, s_{23}=2.3 mm, s_{12}=1.3 mm, and d=0.1 mm. The layout of the filter is shown in Fig. 11, while the photograph of the fabricated circuit is shown in Fig. 12. The overall size of the filter is only 0.385λ_g x 0.34λ_g, where λ_g denotes guided wavelength.

The simulated and measured responses of the filter are compared in Fig. 12, where the specified transmission zeros near the edges of the passband can be clearly identified. A good agreement between the measured and simulated responses can be observed, except for a shift in frequency approximately equal to 1.4 %: the measured central frequency is 2.88 GHz. Since manufacturer specifications for substrate material allow variations in the range ±0.5, as well as variations of substrate thickness, this can be explained by the discrepancy between the actual and simulated values of the dielectric constant and the substrate thickness. For a better comparison of the responses, a normalized frequency axis is used in Fig. 12.

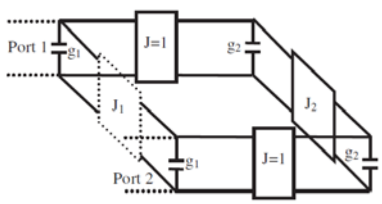

Figure 10. Generalized equivalent network of the proposed filter, [5]

V. Conclusions

In this paper, modified square grounded patch resonator was presented and used in the design of cross-coupled bandpass filters. The filter synthesis procedure is shown in detail. To demonstrate the potential of the grounded patch resonator and this approach, a cross-coupled bandpass filter of the fourth order has been designed, fabricated and measured. The filter is characterized by compact dimensions, equal to 0.385λ_g x 0.34λ_g, where λ_g denotes guided wavelength. In addition, it exhibits stopband rejection up to 8GHz, as well as small sensibility to resonator offset and fabrication tolerances.

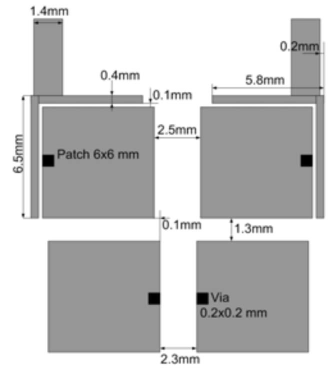

Figure 11. Layout of the filter with all relevant dimensions.

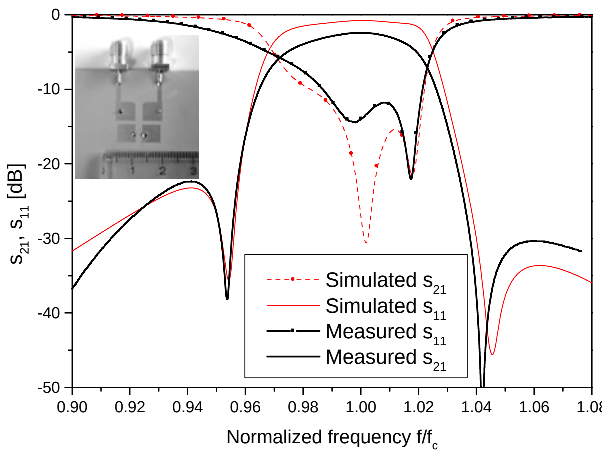

Figure 12. Comparison of simulated and measured responses and the photograph of the fabricated circuit.

References

[1] J. S. Hong: "Couplings of asynchronously tuned coupled microwave resonators," IEE Proc. of Microw. Antennas Propagation, 147, 354, 2000.

[2] R. J. Cameron, General coupling matrix synthesis methods for Chebyshev filtering functions. IEEE Tranc. Microw. Theory Tech. Vol. 47, pp. 433, 1999.

[3] J. S. Hong and M. J. Lancaster, Microstrip filters for RF/microwave applications. New York, Wiley, 2001.

[4] J. S. Hong and M. J. Lancaster, Cross-coupled microstrip hairpin-resonator. IEEE Tranc. Microw. Theory Tech. Vol. 46, No. 1, January 1998.

[5] K. S. Chin and D. J. Chen, Harmonic-suppressing bandpass filter based on coupled triangular open-loop stepped-impedance resonators. Microw. Optical Tech. Lett. Vol. 52, No. 1, January 2010.

[6] P. Jarry and J. Beneat, Design and realizations of miniaturized fractal RF and microwave Filters. New Jersey, John Wiley, 2009.

[7] D. Sievenpiper, L.. Yhang, R.F.J. Broas, N. Alexopulous, and E. yablanovitch, High-impedance electromagnetic surfaces with a forbidden frequency band. IEEE Tranc. Microw. Theory Tech. Vol. 47, No. 11, November 1999.

[8] V. Radonić and V. Crnojević-Bengin, Super-compact stopband filter based on grounded patch resonator," *Electronic lett.*, Vol. 46, No.2. pp.146-147, Januar 2010.

[9] V. Radonić, V. Crnojević-Bengin and B. Jokanović, Novel left-handed unit cell for multi-band filtering applications. European microwave conference 2008, Amsterdam 2008.